SARAF SUPERCONDUCTING MODULE COMMISSIONING STATUS

A. Perry, D. Berkovits, I. Gertz, I. Mardor, J. Rodnizki, L. Weissman Soreq NRC, Yavne, Israel
K. Dunkel, M. Pekeler, C. Piel, P. vom Stein, D. Trompetter Research Instruments GmbH, Bergisch Gladbach, Germany
B. Aminov, Cryoelectra GmbH, Wuppertal, Germany

Abstract

The accelerator at Soreq Applied Research Accelerator Facility (SARAF) is a 176 MHz linac, currently under commissioning at Soreq NRC. Phase I of the accelerator includes a Prototype Superconducting Module (PSM) containing 6 half wave resonators (HWR).
PSM commissioning over the last year included:

a. Pulsed RF and Helium processing, successfully reducing field emission.
b. Extensive investigation of microphonics sources in the PSM, including a study of the piezoelectric and stepper motor tuning systems.
c. Beam operation. A 2 mA pulsed proton beam has been accelerated by the resonators up to 3.7 MeV. Several diagnostic instruments were used to characterize the output beam.

INTRODUCTION

The SARAF accelerator is a linear, high current, 176 MHz RF accelerator designed for acceleration of 2mA proton and deuteron beams up to 40 MeV [1]. Currently, phase I of the accelerator is under commissioning at Soreq NRC [2] by RI Research Instruments GmbH [3] and Soreq NRC [4]. Phase I facility is illustrated in Figure 1.

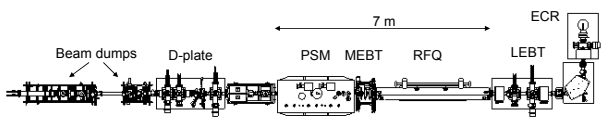

Figure 1: Overview of Phase I of SARAF accelerator.

The PSM (designed and manufactured by ACCEL/RI, [5, 6]) is the first of 6 superconducting modules, containing a total of 44 half wave resonators. Inside the first cryostat are 6 β=0.09 cavities made of bulk Nb, designed to provide acceleration of the particles from 1.5 MeV/u to approximately 5 MeV. In addition, the PSM houses 3 superconducting solenoids for transversal focusing.

HE PROCESSING

The total cryogenic loss at 4.5 K is expected to be lower than 70 Watts at the cavities' design gradient, equivalent to a peak electric field of 25 MV/m. The above value is the sum of the static and dynamic losses in the cryostat. The dynamic losses should not exceed 10 Watts per cavity (Q_0>4.7×10^8).
After fabrication, all cavities were tested individually in a cavity test stand where the unloaded Q values were extracted from RF measurements for different field values [5]. As can be seen in Table 1, all cavities performed in accordance with their design value in the cavity test.

Table 1: Cavity RF Losses at 4.5 K: at the cavity test, before and after pulsed RF and He processing (on site). Before processing, high losses disabled measurements for cavities 4 and 6 at 25MV/m.

Cavity#	Cavity Test [W]	Before Processing [W]		After Processing [W]	
	25 MV/m	20 MV/m	25 MV/m	20 MV/m	25 MV/m
1	7.3	1.9	7	2.2	5.5
2	7.3	3.0	6.3	4.8	8.7
3	6.3	12.3	16.8	7.0	14.8
4	6.3	11.1	---	3.9	10.6
5	5.5	5.4	15.1	3.3	8.8
6	7.3	9.6	---	5.4	10.7
total	40	43.3	---	26.6	59.1

On site measurements were done by estimation of the cryogenic losses from the measurement of the He supply flow. These measurements showed higher losses than previously measured for some of the cavities at the cavity test. The increase in loss between 20 and 25 MV/m and the high radiation levels detected (Fig. 2, bottom) both gave clear indication for the onset of field emission. High power pulsed RF processing up to a peak field of 43 MV/m, using a phase locked loop (PLL) setup did not improve the performance.

At that point it was decided to try Helium processing for cavities 3, 4 and 6. The cavities were filled with high purity helium gas (99.9999%), to a pressure of 4×10^{-5} mBar. The PLL was used to apply high power pulses (43 MV/m in peak field) with 5 Hz repetition and about 20 msec length. Each cavity was processed for several hours, until no more processing events were observed and the radiation level was stable.

After He processing the losses were measured again. Significantly reduced levels of radiation were measured for the processed cavities (Fig. 2, top). Further decrease in

radiation was observed after the Helium was completely evacuated. Slight differences in loss values may be attributed to measurement uncertainty including cryogenic loss estimation and field calibration error, totaling in a few watts. A possible explanation for the increase in loss for cavity 2 may be some remnant surface contamination from the He processing. While only three cavities were He processed, all six were filled with gas.

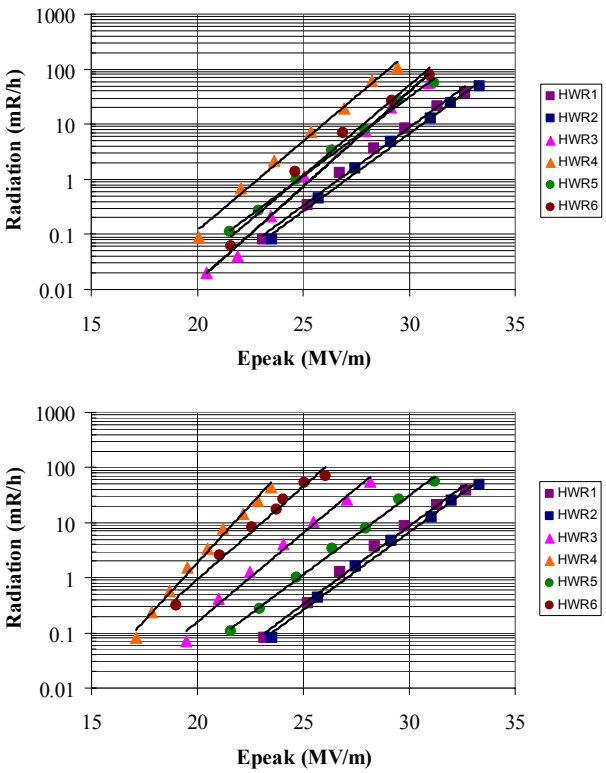

Figure 2: Radiation levels before (Bottom) and after (Top) Helium processing of cavities 3, 4 and 6. Radiation was measured by a γ detector ~ 3 m perpendicular to the PSM.

MICROPHONICS AND TUNER ANALYSIS

The half wave resonators are fairly sensitive to fluctuations in the He pressure. The ± 1.5 mBar stability of the cryogenic system is reflected by frequency detuning exceeding the cavities loaded bandwidth of 130 Hz, since their sensitivity is approximately 60 Hz/mbar. This places some stringent demands on the cavities tuners.

The tuner used at SARAF phase I is illustrated in Figure 3. It is composed of a stepper motor (SM) used for coarse tuning and a piezoelectric element for fine tuning.

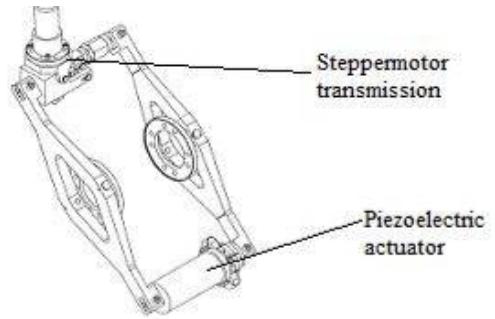

Figure 3: Drawing of the tuner.

From tests of the piezo reaction it became apparent that some of the piezoelectric elements suffer from a reduced tuning range and electrical capacitance (Table 2). At first it was suggested that a depolarization of the elements had happened due to accidental application of reverse voltage at room temperature. A procedure for re-polarization of the crystals was attempted, without success.

It was then speculated that the piezos may have suffered from a mechanical malfunction. This could have an effect over the mechanical boundary conditions of the cavities, thus also accounting for an observed difference in stability between cavities. In an effort to understand the problem a few tests were conducted, described hereafter.

The cavity-tuner system is designed to operate under expansion over its whole tuning range. If this is not the case, backlash phenomena may occur. Therefore, the stepper motor was moved from its zero point to the limit of its travel range (Fig. 4). The piezo tuning range was then measured at different stepper positions, as well as the cavity's resonance frequency. If indeed at some point the tuner will no longer operate against the cavity's expansion, a deviation from linearity is expected. In addition, the piezo tuning range should noticeably change in this case.

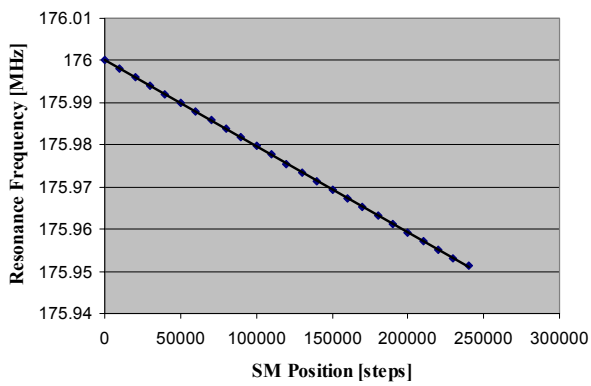

Figure 4: Cavity 5 resonance as a function of SM position.

It can be seen that the cavity resonance frequency changes linearly with the change of SM position over half of its stroke, equal to ~0.3 mm. In addition, no distinct change in the piezo tuning range was observed.

After the above measurements the cryostat was warmed up and opened, and the piezo elements were exchanged. An analysis performed by the manufacturer (Piezomechanik GmbH) revealed that four of the six piezoelements suffered from loose electrical contacts. The lost contact was probably due to differential thermal expansion. The design was modified by piezomechanik to prevent recurrence of the problem.

Table 2: Piezo tuning ranges for the six cavities, before and after the exchange of the piezoelements.

Cavity#	July 09 [Hz]	August 09 [Hz]
1	536	900
2	866	780
3	806	1013
4	794	978
5	448	874
6	919	1384

The PLL control system was applied to measure the microphonics spectrum of all six resonators. This was done by measuring the control voltage of the Voltage Controlled Oscillator, which follows the resonance frequency of the cavity. Figure 5 demonstrates a measured microphonics spectrum for one of the half-wave resonators. Mechanical modes around 50Hz and at 150 Hz were common to all cavities, in addition to the sub Hz component originating from He fluctuations (Fig. 5). Analysis of the histogram and autocorrelation functions indicated that these modes were probably excited by broadband noise [7,8].

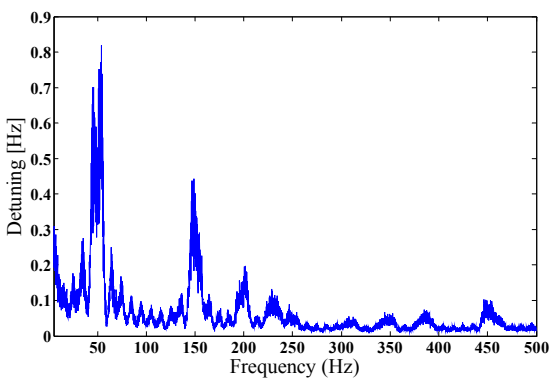

Figure 5: Resonator 1 microphonics spectrum. Only modes above 5Hz are shown.

In order to identify sources of microphonics, piezoelectric sensors have been placed at different locations outside the cryostat. Figure 6 presents two microphonics spectra measured on the He supply line (green) and cryostat bottom (blue). Unfortunately, the equipment was sensitive to electrical noise coming from the 50 Hz mains. Therefore, the 50, 100 and 150 Hz peaks (seen on both curves) can not be directly identified as microphonics resonances. However, the peaks were still present, to a less extent, when the same spectrum was taken during a power break.

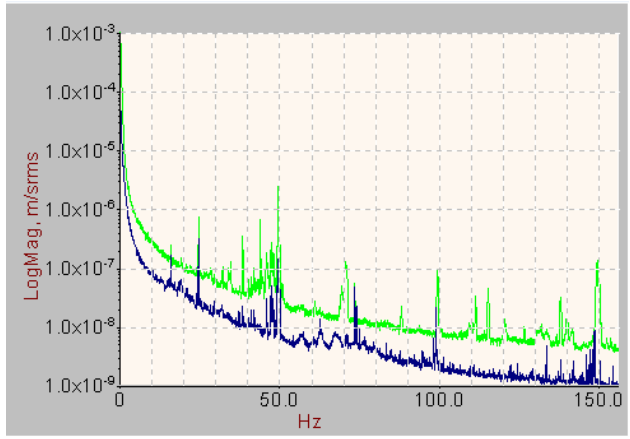

Figure 6: Measurement of mechanical vibrations on the He supply line (green) and cryostat bottom (blue).

BEAM OPERATION

A 2 mA pulsed proton beam was accelerated through the RFQ and PSM. The pulse repetition rate was set to a few Hz and the pulse length was typically 100 μsec.
The pulsed beam operation had several goals: optimization of RFQ voltage, calibration and phase synchronization of the HWRs, characterization of the beam and comparison with beam dynamics simulations. To complete these tasks several diagnostic instruments were used:

a. Standard slit wire systems for profile and emittence measurements.
b. Phase probes to allow for beam energy measurement by time of flight (TOF).
c. Rutherford Scattering [RS] off a gold foil inserted into the beam halo. Silicon detectors at 45 and 100 degrees record the spectrum of the scattered particles to determine the beam energy [9].

RF-phase synchronisation with the beam for all HWRs was performed by rotating the RF phase and measuring the output energy using TOF or RS [Fig. 7]. The optimal RF phase corresponding to beam dynamics simulations was found and set for each cavity. After the cavity field adjustment, the procedure was repeated for the next cavity.

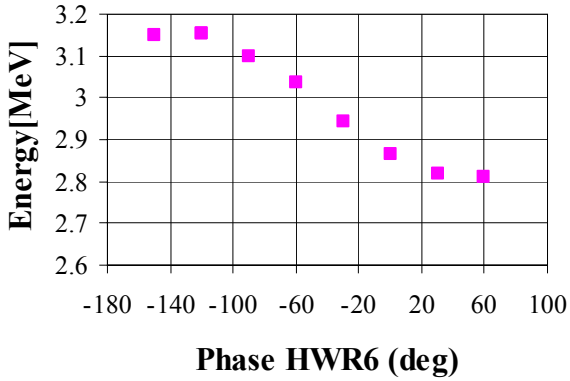

Figure 7: Proton energy as function of HWR6 phase (energy calculated from TOF measurements).

The first two resonators were used for beam bunching, while the last four provided acceleration. The accelerating cavities were operated at voltages between 550kV and 900 kV, in accordance to beam simulations and field stability limits. These voltages are equivalent to peak electric fields of 16 to 27 MV/m. The maximal beam energy obtained by this setup was 3.7 MeV (Fig. 8). The source of the systematic difference between TOF and RS results is still under investigation. RS measurements were calibrated by the RFQ output energy (1.5 MeV). The estimated error of the TOF measurement is in the range of 10 – 40 keV.

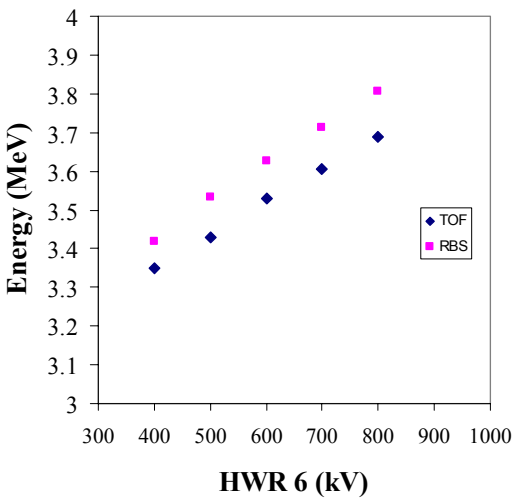

Figure 8: Proton energy versus HWR6 voltage, from TOF [blue] and Rutherford scattering [pink] measurements.

The phase probes and Rutherford scattering measurements provide additional information about beam bunching. The phase probe signal amplitude is dependent on the longitudinal bunch length, while the Rutherford scattering spectrum is a straightforward measurement of the beam energy spread. Thus, it was possible to determine the effectiveness of cavity 6 when used as a buncher by looking at the Rutherford spectra [Fig. 9]. At that point cavities 4 and 5 were not operating.

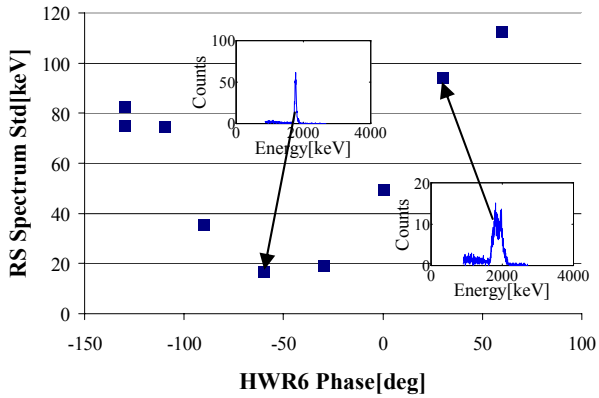

Figure 9: Width of the RS spectrum for different phases of cavity 6. Also displayed are two RS energy spectra: for 30 and -60 degrees.

SUMMARY AND OUTLOOK

Several steps had been taken towards the commissioning of SARAF PSM over the last year. Beam operation with the superconducting cavities had demonstrated some progress as well as good agreement with beam dynamics simulations. However, control and stability of the RF fields in the resonators should be improved. Some problems in the electronics were already identified, and the endeavour will resume in the coming months.

We wish to express our acknowledgment to Asher Grin for the operation of the cryogenic system and to Yossi Eisen for the development of the RS monitor.

REFERENCES

[1] A. Nagler et al., “Status of the SARAF Project”, LINAC'06, Knoxville, August 2006, MOP054, p. 168 (2006).

[2] http://www.soreq.gov.il/default_EN.asp

[3] http://wsww.research-instruments.de/, a former Accel Instruments GmbH activity.

[4] I. Mardor et al., “Status of the SARAF CW 40 MeV Proton/Deuteron Accelerator", PAC May 4-9, 2009, Vancouver, Canada, FR5REP087

[5] M. Pekeler et al., “Development of a Superconducting RF Module for Acceleration of Protons and Deuterons at Very Low Energy”, LINAC'06, Knoxville, August 2006, TUP034, p. 321 (2006).

[6] M. Pekeler et al, "Design of a Superconducting Half Wave Resonator Module for Proton/Deuteron

Acceleration", SRF'03, Travemünde/Lübeck, September 2003, MoP36 (2003).

[7] J.R. Delayen, "Pondermotive instabilities and microphonics – a tutorial", Physica C 441 (2006) 1-6, May 2006.

[8] C. Piel et al., "Phase 1 Commissioning Status of the 40 MeV Proton/Deuteron Accelerator SARAF", EPAC'08, Genoa, June 2008, THPP038, p. 3452 (2008).

[9] L. Weissman et al., " First Experience at SARAF with Proton Beams using the Rutherford Scattering Monitor", DIPAC'09, Basel, May 2009, TUPB20 (2009).